



Storm-induced sediment supply to coastal dunes on sand flats

Filipe Galiforni Silva¹, Kathelijne M. Wijnberg¹, and Suzanne J.M.H. Hulscher¹

¹Water Engineering & Management, Faculty of Engineering Technology, University of Twente, P.O. Box 217, 7500 AE, Enschede, The Netherlands

Correspondence: Filipe Galiforni Silva (f.galifornisilva@utwente.nl)

Abstract. Marine supply of sand can control the development and morphology of coastal dunes. However, processes that control the sediment transfer between sub-tidal and the supra-tidal zone are not fully understood, especially in coastal settings such as sand-flats close to inlets. It is hypothesised that storm surge events induce sediment deposition on sand-flats, so that this may influence dune development significantly. Therefore, the objective of this study is to identify which processes causes deposition on the sand-flat during storm-surge conditions and discuss the relation between the supra-tidal deposition and sediment supply to the dunes. We use the island of Texel as a case study, on which multi-annual topographic and hydrographic data sets are available. Additionally, we use the numerical model XBeach to simulate the most frequent storm surge events for the area. Results show that supra-tidal shore-parallel deposition of sand occurs in both the numerical model and the data. The amount of sand deposition is directly proportional to surge level, and can account for more than half of the volume deposited at the dunes on a yearly basis. Furthermore, storms are also capable of remobilising the top layer of sediment of the sand-flat, making fresh sediment available for aeolian transport. Therefore, in a sand-flat setting, storm surges have the potential of adding significant amounts of sand for aeolian transport in periods after the storm, suggesting that storms play a significant role in the onshore sand supply between sub-tidal and subaerial zones in those areas.

1 Introduction

Coastal dunes are important natural flood defence features. Dunes grow in the interface between land and sea by interaction of biological, physical processes and geological conditioners (Hesp, 1983; Sherman and Bauer, 1993; Hesp, 2002; Bauer and Davidson-Arnott, 2002; Hesp and Walker, 2013; Delgado-Fernandez and Davidson-Arnott, 2011; van Puijenbroek et al., 2017). Generally, key aspects necessary for the development of coastal dunes are: availability of sediment, space for dune growth, suitable climate conditions (e.g. wind, waves, vegetation, rain, etc) and time for its development (Hesp, 1983, 2002; Bochev-van der Burgh et al., 2009; Bauer et al., 2009; Bochev-Van der Burgh et al., 2011; Keijsers et al., 2015; van Puijenbroek et al., 2017; Silva et al., 2018, 2019).

The amount of available sediment is a key aspect for dune development (Eastwood et al., 2011; Hesp, 2002; Short and Hesp, 1982; Houser, 2009). It can control aspects like dune type and morphology, vegetation growth and overall development. The sea is the main source of sediment for coastal dunes. Wave-driven currents, oscillatory components of the incident wave motions and effects of infra-gravity waves on currents are responsible of transporting sediment onshore, leading to a continuous supply of sediment from the sub-tidal to the subaerial zone (Aagaard, 2014). Aagaard et al. (2004) link the occurrence of onshore bar



migration and its subsequent welding to the coast with sediment supply towards the dunes. Anthony et al. (2006) show that, for a tide-dominated beach in the coast of France, dune accretion on a yearly basis depends on bar welding phenomena related to storm processes, which could account for 48% of the overall dune change. Anthony (2013) shows that for the southern North Sea coastal system (i.e. French and Belgium coast), the highest rate of foredune accretion is associated with areas where sand banks have migrated onshore in the past century, thus leading to an increased supply condition for the dunes.

Most studies on beach-dune systems and sediment transfer between sub-tidal and supra-tidal zones only consider locations away from inlets (Anthony et al., 2006; Anthony, 2013; Aagaard et al., 2004; Reichmüth and Anthony, 2007). Inlet-driven processes such as shoal attachment and channel migration can drive changes in the adjacent coastlines (Fitzgerald et al., 1984; Fenster and Dolan, 1996; Robin et al., 2009; Elias and Van Der Spek, 2006), which in turn can influence sub-tidal/sub-aerial sediment exchange and coastal dune behaviour (Ruessink and Jeuken, 2002; Aagaard et al., 2004; Anthony et al., 2006; Cohn et al., 2017). Furthermore, inlet-driven processes can define the overall shoreline shape, which can favour or disfavour the development of dunes. For barrier islands in the Dutch Wadden sea region, coastline stretches close to inlets commonly develop as sand flats due to long-term morphodynamics of its ebb-tidal delta systems, as illustrated by the example of De Hors in the Texel island (The Netherlands) (van Heteren et al., 2006; Elias and Van Der Spek, 2006). Those sand flats are large (scale of km) and present great potential for dune growth due to their large beach width, prevailing wind velocities, and climate (Bauer et al., 2009; Houser and Ellis, 2013). Recent analysis of annual topographic data (Wijnberg et al., 2017) suggested that supra-tidal storm deposits may form a source for sand supply towards the dunes. However, it is unclear during which conditions supra-tidal deposition occurs and whether the amount deposited can be considered significant for dune growth and development.

Therefore, the objective of this study is to identify processes and storm properties that causes deposition on the sand-flat during storm-surge flooding and discuss the relation between the supra-tidal deposition and sand supply to the dunes. We use a site in the Netherlands (Texel island) as a case study, for which we analysed multi-annual topographic data sets together with the application of a numerical model to investigate bed level changes at the sand flat during storm-surge flooding events.

The paper outline is as follows: Section 2 shows the study area characteristics; Section 3 shows the available data, its treatment and usage and explains the numerical model, its concepts, initial conditions and assumptions. Section 4 presents the results separated by data analysis, field survey and numerical results, followed by a discussion section (5) and conclusion (6).

2 Study area

On the southern side of the Texel island (The Netherlands), bordering the Marsdiep Inlet, long-term ebb-tidal dynamics built a sand flat (named "De Hors") where dunes have been emerging over the past 20 years, at least (Figure 1). The flat has an approximate area of 3 km^2 . According to Silva et al. (2018), around $1.2 \cdot 10^6 \text{ m}^3$ of sand has been deposited in the dunes between 1997 and 2015. Furthermore, dunes can be separated in three distinct zones: a western part, more exposed to wave action, a central zone, and an eastern part, which receives less wave action. According to Silva et al. (2018), the western zone accounted for 60% of the total dune volume increase, which emerged mostly as a linear dune ridge, similar to foredunes found



along the coast away from the inlet. The central dune zone accounted for about 30% of the total dune volume increase, and emerged as coppice-like dunes. The eastern zone presented the lowest dune volume increase, and evolved as a linear dune ridge.

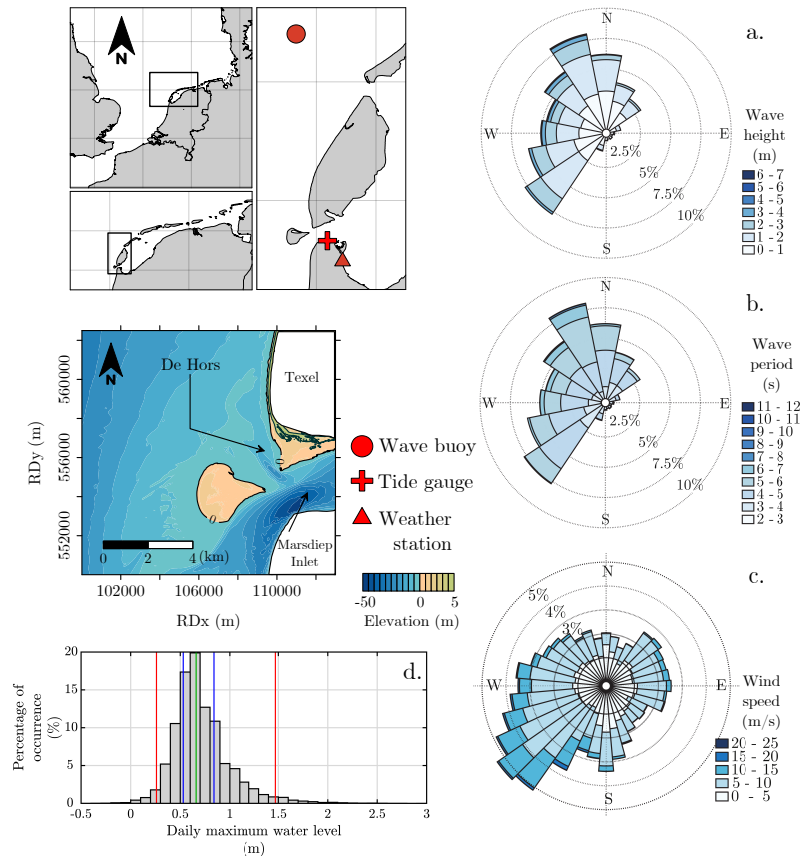


Figure 1. Study area of Texel. Red symbols represent the locations of the wave buoy (circle), weather station (triangle) and tide gauge (cross) used in this paper. Directional histograms for Wave Height (a.), Wave period (b.) and Wind speed (c.) show the overall characteristics of the area for wave climate and wind direction. Histogram of daily maximum water levels (d.) has also been plotted, with the blue lines representing the 25 and 75 quartiles (mean spring high tide, approximately), and the red lines 2.5 and 97.5 limits.

The Marsdiep inlet can be classified as a mixed-energy wave dominated inlet, with a gorge width of 3 km and a channel depth up to 50 meter (Elias and Spek, 2017). The inlet has an asymmetric ebb-tidal delta that is largely conditioned by side-effects due to engineering projects (i.e. construction of the "Afsluitdijk") (Elias and Van Der Spek, 2006; Elias and Spek, 2017). The sand flat is exposed to wind most of the times and is flooded only during storm surge conditions. The main wind direction is from southwest, whereas waves predominantly come from southwest and northwest directions (Figure 1). The mean tidal range is 1.34 meters, with a mean spring high tide level (MSHTL) of 0.84 meters.



Table 1. Characteristics of the local storm climate. Occurrence relates to the percentage of occurrence of storms with those characteristics over the population of mild, storm or extreme storms.

Storm	Wave Direction	Wave Height (m)	Period (s)	Occurrence (%)
Mild	SW	2 - 3	5 - 6	17,3
	SW	3 - 4	5 - 6	8,5
	W	2 - 3	5 - 6	5,2
	W	3 - 4	5 - 6	16,7
	W	4 - 5	5 - 6	8,2
	NW	3 - 4	6 - 7	8,8
	NW	4 - 5	6 - 7	14,6
Storm	SW	3 - 4	6 - 7	9,1
	W	2 - 3	5 - 6	6,8
	W	3 - 4	6 - 7	25,0
	W	4 - 5	6 - 7	15,9
	NW	3 - 4	6 - 7	15,9
	NW	4 - 5	6 - 7	11,4
Extreme Storm	W	4 - 5	6 - 7	33,3
	NW	5 - 6	7 - 8	33,3
	NW	5 - 6	8 - 9	33,3

In the present paper, storm is defined by its maximum water level following the classification used by the Dutch Ministry of Infrastructure and Water Management ('Rijkswaterstaat'). Storms with maximum water levels between mean spring high tide and 1.9 meters above MSL are classified as mild, whereas maximum water levels between 1.9 and 2.6 meter above MSL are classified as normal storms, and above 2.6 meters are classified as extreme storm. To determine the local storm climate, we used a time series of hourly water levels collected at a tide gauge in the channel margin together with hourly wave information from a wave buoy (Figure 1). Daily maximum water levels were extracted from the time series and used as proxy for storms. Results show that 73,31% of the daily maximum water levels lie below mean spring high tide level, whereas 26,15% can be considered mild storms. From the mild storms, the majority lies between MSHTL and the 97,5 quartile (22,26%), with only 3,88% representing water levels above the 97,5 quartile. Only 0,54% can be considered storms (0,5%) or extreme storms (0,04%).

Waves related to storms are separated from each storm class (i.e. mild, storm and extreme storm) in Table 1. Mild storms present waves coming from three directions (SW, W and NW), with relatively similar occurrence (25,8%, 30.1% and 23.4%). For storms and extreme storms, waves tend to come from more northern directions.



3 Methodology

To achieve the proposed goal, we take two main approaches: numerical modelling and data analysis. The data analysis is meant to highlight morphological behaviour of the sand flat, focusing on the occurrence of deposition in zones above the MSHTL. Furthermore, data analysis will also deal with a field campaign meant to qualitatively measure the effects of a single storm onto the sand flat. The numerical modelling is used to analyse in depth which processes control the deposition and identify which storm conditions will lead to sand deposition.

3.1 Data and Field Campaign

To analyse beach-dune behaviour over the sand flat area, we used annual LiDAR data from 1997 up to 2018 provided by the Dutch Ministry of Infrastructure and Water Management ('Rijkswaterstaat'). Survey dates vary over the years, with a tendency of flights being done after the most energetic period (Figure 2). The data is available in a horizontal resolution of 5 meters up to 2013, when a finer horizontal resolution of 2 meters became available, with vertical accuracy within 0.08 meters. From the LiDAR data, we analysed changes in elevation and volume of both the dune field and the sand flat. For the present study, the dune area has been defined by the limit threshold contour of 3 meters, whereas the sand-flat area has been defined as the area between dunefoot and mean spring high tide level (i.e. MSHTL). To analyse the stability of the sand flat, we created variance maps using the entire data set. Variance maps show the elevation variance at each grid node, which highlights areas on which elevation changes occurred in a larger magnitude. Furthermore, elevation difference maps have been used to define erosion and accretion trends between surveys. Thus, areas with low growth trend and high variance values means that even though no accretion/erosive trend occurs, the elevation varies considerably in time. Moreover, to determine whether a location presented more accretive or erosive events in time, we built maps of occurrence of accretion and erosion events (i.e. number of times which a certain location had accretion or erosion events larger than 0.15 meters). Thus, areas where more accretive or erosive events happened can be highlighted. Therefore, trend maps are meant to show the overall growth trend of the location, variance maps are meant to show if the location is stable in time regardless its trend, and occurrence maps are meant to show areas where more accretive or erosive events occurred, regardless its variability and trends over time.

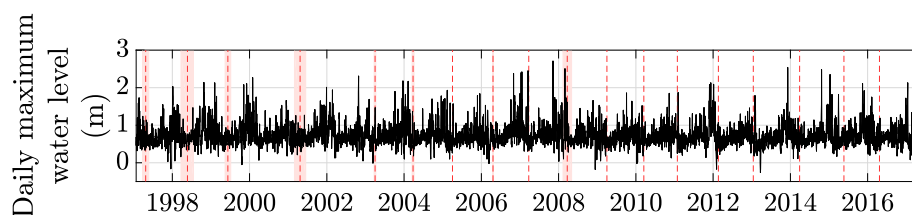


Figure 2. Daily maximum water level time-series highlighting the periods when the topographic surveys were executed. Dashed red lines represent the exact date used in the analysis, whereas the pink-shaded region represent the period during which the measurements were (only for surveys where the exact date were not available).



To analyse the effects of a storm on the surface layer of sediment at the sand flat, we executed a field campaign on January, 2017, where six rods with washers were deployed over the flat to check whether remobilisation of the sand occur and, if so, in which order of magnitude (Figure 3). Elevation data was acquired using an RTK-DGPS system.

Regarding validation of the numerical model, one hydrodynamic dataset was available to assess model performance for the present study. The ferry that links Texel island with the mainland crosses the Marsdiep inlet every half an hour from 6 AM up to 9:30 PM with an Acoustic Doppler current profiler (ADCP) mounted, performing detailed flow measurements. The data, acquired and treated by the Royal Netherlands Institute for Sea Research (NIOZ) has been made available for the year of 2009 by Duran-Matute et al. (2014). One limitation of the data set is that the ferry does not sail at night. Furthermore, the ferry also does not sail when water level exceeds 2 meters above NAP. That would introduce gaps and limit the amount of possible storms for validation to only periods of mild storms. To assess model performance, we use the storm of 04/10/2009, which reached maximum water levels of 1.8 meters and was measured for a period of three hours.

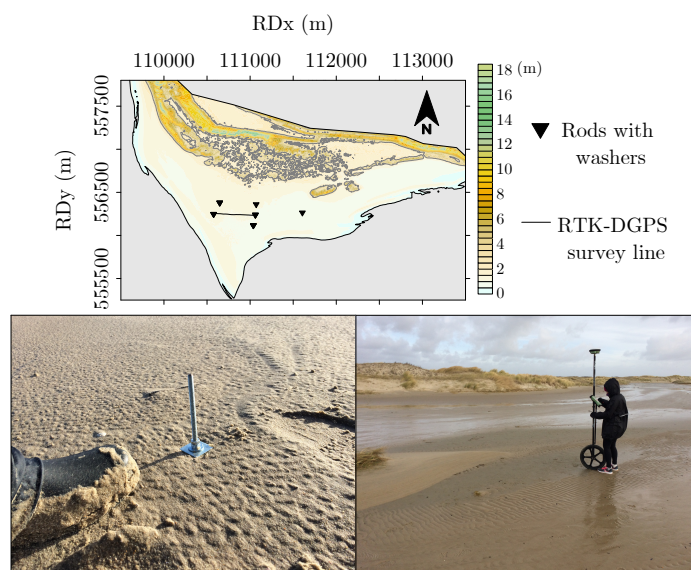


Figure 3. Location of the rods with washers, as well as RTK-DGPS survey transects.

3.2 The XBeach Model

Considering that the available measurements are surveyed in an annual basis, we choose to apply a numerical model using the most frequent storm conditions to identify in which storm conditions does deposition onto the sand-flat occur in an event scale.

15 3.2.1 Model Structure

The XBeach model (Roelvink et al., 2009) is a process-based model developed to simulate hydrodynamic and morphodynamic processes on sandy coasts. It has been developed to work on a time-scale of storms and for coastal stretches of the order of kilometres in length. The model solves the 2D horizontal shallow water equations, including capabilities of time-varying



5 wave action balance, roller energy balance, advection-diffusion equation, sediment transport and bottom change (Elsayed and Oumeraci, 2017; Roelvink et al., 2009; Deltares, 2018). Overall, the model includes the hydrodynamic processes of short-wave transformation (refraction, shoaling and breaking), long wave transformation, wave-induced setup and unsteady currents, as well as overwash and inundation. The morphodynamic processes include bed load and suspended sediment transport, dune face
 5 avalanching, bed update and dune breaching (Deltares, 2018). The main difference of the XBeach model compared to other process-based models for coastal areas is the capability of including the effects of infragravity waves through solving long-wave motions created by time-dependent cross-shore wave height gradients (Roelvink et al., 2009). For the present study, the model has been run in surfbeat mode, where the short wave variations on the wave group scale and the long waves associated with them are resolved (Deltares, 2018). The model has been extensively validated and applied in different scenarios (de Vries, 2009;
 10 Roelvink et al., 2009; McCall et al., 2010; Elsayed and Oumeraci, 2017; Vet, 2014; Nederhoff, 2014). Detailed information on model formulation and validation can be found on Roelvink et al. (2009) and Deltares (2018).

3.3 Scenarios

Based on the local storm climatology (Table 1), we selected 12 actual storms events that occurred between 1990 and 2017 to represent the most frequently occurring storm conditions in each of the three storm categories. Choices have been made
 15 to ensure that we simulate at least one storm from each wave direction represented. The bathymetry and topography for all scenarios are based on LiDAR and bathymetric data available for the year 2009, the same year of the storm chosen for validation, thus only hydrodynamic boundary conditions have been changed for each scenario. Bathymetric data is available at 20x20 meter grid, with vertical accuracy between 0,11-0,4 meters, whereas topographic LiDAR data is available at 5x5 meter grid, with vertical accuracy within 0.08 meters. For each storm, its wave characteristics have been gathered from data available
 20 from a nearby wave buoy (Figure 1). Final scenarios are shown in Table 2.

From the simulations, we relate bed level change on the flat with local hydrodynamic characteristics (i.e. H_{rms} , u and v convergence, S_{xx} , S_{xy} , S_{yy}), in order to check which process would explain most of the bed level change. We do this by analysing how the morphology and hydrodynamic evolve in time, by choosing a location where deposition occurs and following the time-series of bed level change and hydrodynamic processes. Furthermore, to check if storm strength influences the amount
 25 of deposited volume onto the sand flat, we correlate final sand volumes deposited with imposed storm characteristics (i.e. Maximum water level imposed at the boundary, H_{m0} , wave direction and T_p). Both sand volume and hydrodynamic variables are standardised using z-scores to ensure that standard deviations are comparable.

3.3.1 Validation

Considering that the XBeach model has been validated in a large range of applications, we use default settings for the present
 30 study. Additionally, we used the above-mentioned dataset for a limited validation check.

Validation results show relatively good agreement between measured and simulated currents, with root mean square error (RMSE) values below 0.5 m/s. Best fit is associated with meridional components (i.e. perpendicular to the inlet throat), with



Table 2. Characteristics of the simulated scenarios. Deposited volume refers to the deposited sand onto the sand flat from the simulation results.

Scenario	Date	Duration simulated (hours)	H_{m0}	Dir	T_p	Max. Water Level	Deposited volume (m^3)	Storm class
a.	25-26/10/2005	8	3,0	235	5,6	1,7	474	Mild
b.	1/10/2008	7	3,0	258	5,3	1,7	1198	Mild
c.	29/10/2017	8	3,8	310	6,4	1,7	7084	Mild
d.	23/11/2009	8	2,9	253	5,4	1,9	7339	Mild
e.	04/10/2009	8	3,8	297	6,3	2,1	14680	Storm
f.	25/10/1998	8	4,0	292	6,5	2,4	15322	Storm
g.	21/12/2003	9	5,8	350	8,1	2,5	26958	Storm
h.	27/10/2002	9	3,5	247	6,2	2,6	10717	Storm
i.	30/01/2000	9	3,6	298	6,7	2,6	16173	Storm
j.	22/10/2014	9	4,7	323	7,1	2,8	19363	Extreme Storm
k.	09/11/2007	10	5,8	337	8,1	3,0	29863	Extreme Storm
l.	26/02/1990	10	5,0	285	7	3,2	18601	Extreme Storm

a R^2 of 0.63 and RMSE of 0.17. For the zonal components (i.e. parallel to the inlet throat), the model underestimated values, specially when the flow presented high velocities, with R^2 of 0.51 and RMSE of 0.41 (Figure 4).

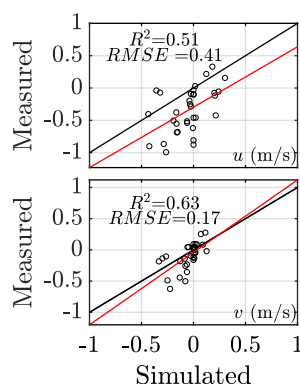


Figure 4. Validation results. Comparison of zonal and meridional components of the depth-averaged flow between simulated and measured data. The location of each point is defined by the ferry location at the time of the measurement and paired with the simulation accordingly. R-squared and RMSE are displayed for in the upper part of each scatter plot. Black line is a diagonal reference line (i.e. from (-1,-1) to (1,1), whilst red line represent the least-squares lines.)



4 Results

4.1 Supra-tidal development

Figure 5 presents elevation difference maps between each year individually. Maps show that deposition patterns in the supra-tidal zone occur between at least 10 different years. For some years like between 1998-1999 and 2003-2004, the deposition happens extending from the north to the south of the flat, and it happens at least 100 meters landward of the mean spring high tide level (i.e. higher elevations). For other periods like (j., l. and r.), the deposition happens much closer to the MSHTL, although also oriented from north to south. For others, the deposition occurs only in the southern tip of the flat, like m. Erosion patterns higher than 0.15 meters occur only between a few years, and mostly at locations close to the MSHTL. When looking at the map of accretion/erosion occurrence (balance of occurrence of accretion and erosive trends between years - Figure 6b), we can also see that a zone with more accretive than erosive years occur in a well formed shore-parallel shape above MSHTL. Thus, we conclude that there is a zone of sediment deposition in the west margin of the flat above mean spring high tide level.

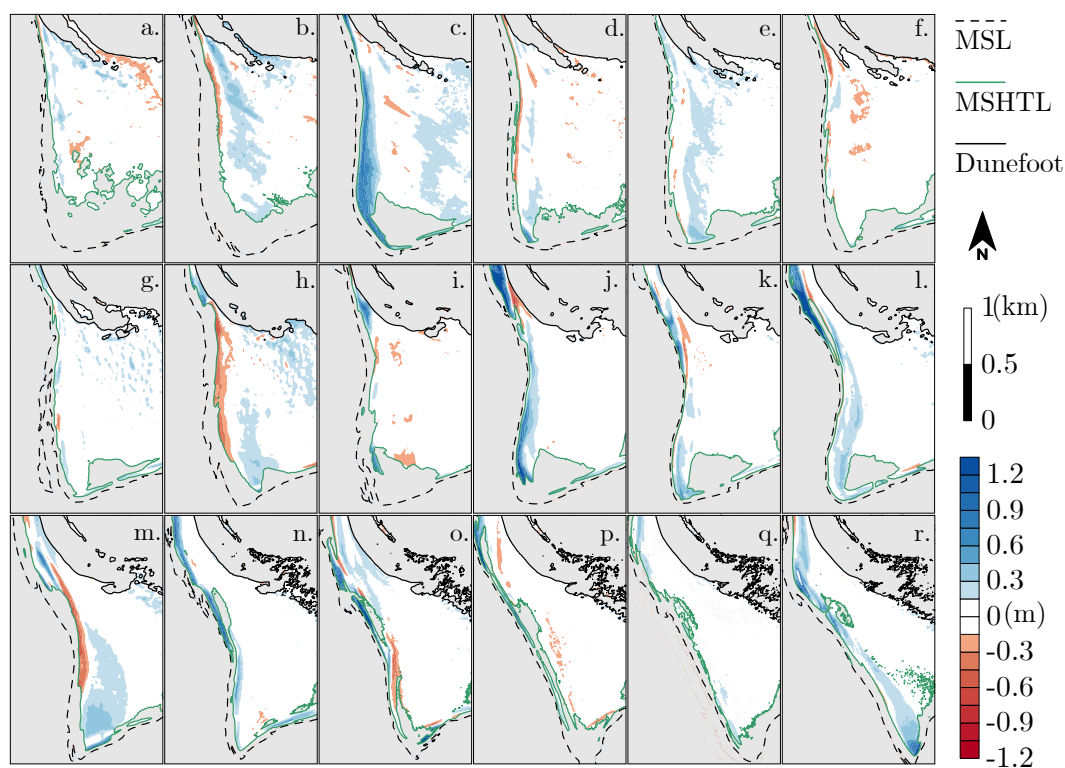


Figure 5. Difference maps for the periods between 1997 and 2017 focusing on the supratidal area. Calculations are done using the next minus the previous survey. Most plots show the an one-year difference, with exception of plots c and d which represent the difference between 1999-2001 and 2001-2003, respectively, due to the absence of surveys in the years 2000 and 2002.

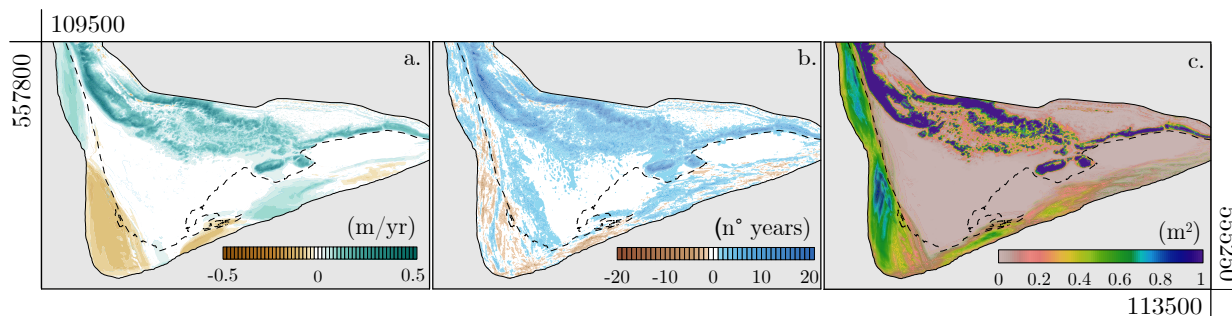


Figure 6. a - Average annual elevation change based on LiDAR data from 1997 up to 2017. Dashed lines show the average position of the MSHTL. b - Net accretion/erosion occurrence of events greater than 0.15 meters. c - Variance of the elevation.

In terms of volume, the supra-tidal depositional zones account for values in the order of $10^4 m^3$, with average values of $6.4 \cdot 10^4 (\pm 4.4 \cdot 10^4) m^3$ over surveyed period, and maximum numbers reaching values one order of magnitude higher (Figure 7). Deposited volume over the sand flat shows no correlation with either maximum water levels or median values of storm surge levels between surveys.

- 5 Even though there is a deposition zone, the flat does not present any growth or erosive trend between MSHTL and dunefoot, suggesting a low elevation variability in a year to year basis. Figure 6a shows the average year to year elevation change. In the upper part, accretion trends relate to dune growth, with elevation change up to 0.5 meter per year. Also, regions of accretion and erosion on levels below mean spring high tide level (MSHTL - dashed lines) range to values between -0.25 and 0.25, approximately. Average annual elevation change in the central part of the flat is minimal, with values within the measurement
- 10 error. Variance maps related to the elevation between each year (Figure 6c) also show that values are greater for sub-tidal zones and zones where dunes have been growing compared to the center of the sand-flat, which has variance values smaller than 0.01 for most of the zone. This suggests that not only average values are close to 0, but also values have been similar, with low variability and small deviation. Thus, to maintain the rate of change close to 0, erosive years must be higher in magnitude than accretive years. Moreover, the location above mean spring high tide level means that either the deposition is caused by water
- 15 levels above mean spring high tide level or by other transport agents like Aeolian transport.

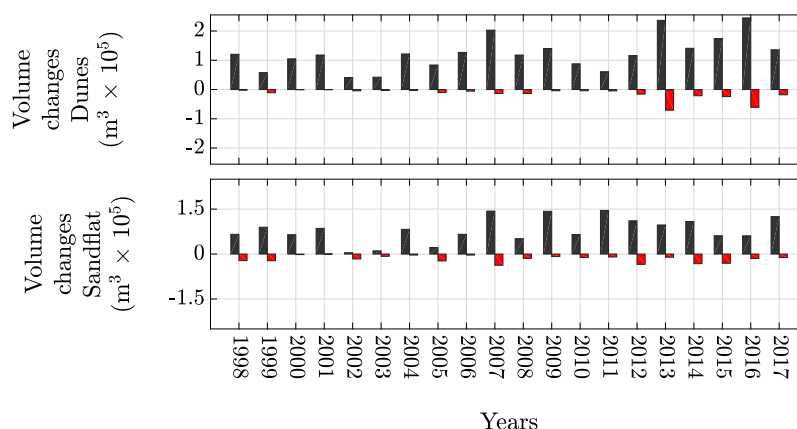


Figure 7. Annual volume changes for the sand flat and dune area considering only cells which change were greater than 0.15 meters (approximately the maximum possible error based on the allowed error for each LiDAR survey.)

Regarding dune growth, on average $1.1 \cdot 10^5 (\pm 4.4 \cdot 10^4) m^3$ of sand per year is deposited on the dunes, which represents a change in height of 0.28 meters per year in average. Overall, a total of $2.3 \cdot 10^6 m^3$ of sand has been deposited in the dune part between 1997 and 2017. This sediment resulted in an average increase in elevation of 2.51 meters and an expansion of the dune field by $9.2 \cdot 10^5 m^2$. Potentially, when comparing the volume of sand deposited at the sand flat and at the dunes, the yearly average volume deposited on the sand flat over the years represents roughly 59% of the yearly average volume change of the dunes.

Results from the field survey show that expressive bed forms (average height of 11 centimetres and length of 150-250 centimetres, approximately) developed on the west portion of the sand flat, gradually diminishing their size towards the east, where they disappeared (Figure 8). This suggests that a decrease in flow velocity occurred from west to east. This also suggest that the top of the sand flat was reworked, with elevation change occurring in almost all rods, with values being higher in the western part due to the bedforms. (Figure 8).

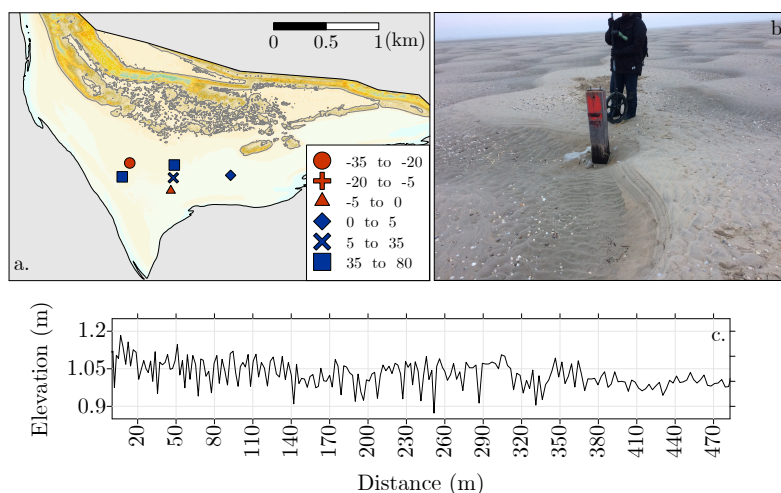


Figure 8. a. Results from the survey, showing the change in surface elevation over the storm flooding event, in cm; b. Picture showing and example of bed form developed after the storm at the sand flat; c. Elevation data along the transect shown on Figure 3 showing the bed forms formed during the storm event of January/2017.

4.2 Modelled scenarios

Simulation of the storm surge events show that deposition above the MSHTL happened in almost all scenarios tested. For most scenarios, the sediment is deposited in a clear shore-parallel north-south deposition patch, with volumes varying from $0.7 \cdot 10^4$ up to $3.10^4 m^3$ of sand. The maximum deposition values occurred for storms h and i, which are labelled as extreme storms (Figure 9). Only two storms did not yield a significant deposition pattern at the sand flat above MSHTL (storms a and b, Table 2), with volume values of $474 m^3$ and $1198 m^3$ deposited over $2320 m^2$ and $6203 m^2$, respectively. These values are distributed in small patches over the plain. Values found in the simulations for the shore-parallel supra-tidal deposition are of the same order of magnitude as the ones derived from the LiDAR data.

Furthermore, simulation results suggest that the amount of sediment deposited tends to be higher for stronger storms. The amount of deposited sand over the sand flat shows a positive correlation ($R > 0.8$) with hydrodynamic forcing conditions ($Hm0$, Tp , dir and $W.L$) (Figure 10). Considering that higher water levels and wave energy are associated with stronger storms, positive values of correlation suggest that stronger storms would lead to more deposition at the sand flat. Even though correlation with main wave direction is also positive, the presence of deposition for all directions suggest that high correlation values are due to the relation between wave energy and wave direction rather than a leading mechanism towards more deposition onto the sand flat.

We further analyse the relation between hydrodynamic processes and morphological evolution along a cross-shore transect for scenario k analysing the time evolution of 7 parameters: local water level, wave height, cumulative bed level change, bed level change, bed level, convergence values of u in the cross-shore direction (i.e. perpendicular to the shoreline) and zonal



components (u) of the flow (Figure 11). We also extracted a time-series from a point in the sand flat where deposition occurred and followed the evolution of water level, wave height, convergence values of u in the cross-shore direction (i.e. perpendicular to the shoreline) and cumulative erosion/accretion (Figure 12).

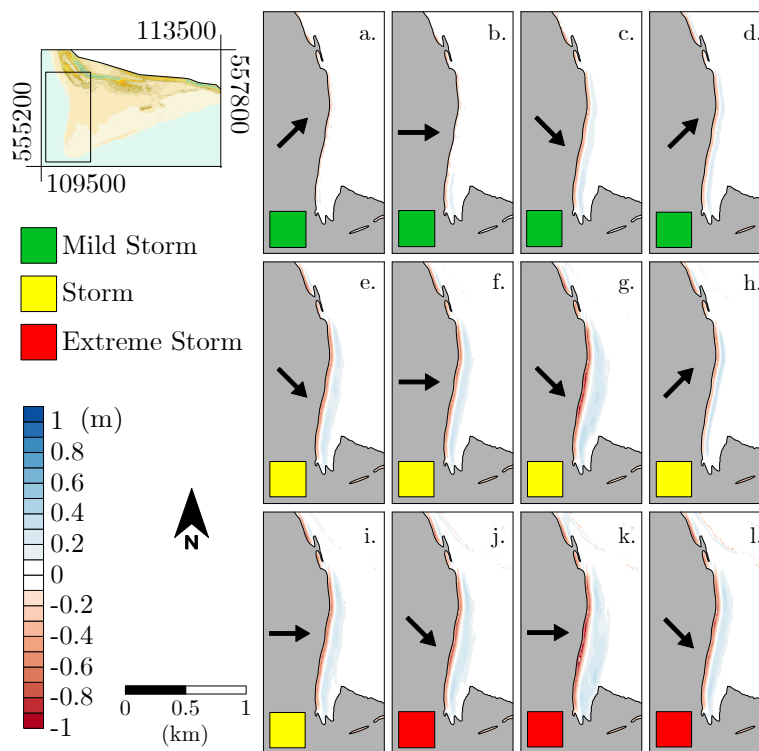


Figure 9. Final elevation change after XBeach simulation for all tested scenarios. Arrows represent the main wave direction for the period, whereas the coloured box shows the storm strength.

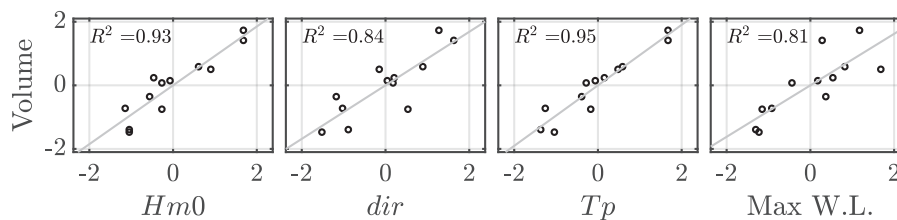


Figure 10. Scatter plot based on zscores for the initial boundary conditions used for each scenario ($Hm0$, Tp , dir and maximum water level) against total volume deposited onto the sand flat.

Regarding currents, Figure 11g. shows the cross-shore component of the depth-integrated currents. Before inundation of the sand flat, the system is dominated by an offshore directed current, related to the formation of an undertow current to



compensate onshore directed wave-driven mass fluxes. As water inundates the flat, the offshore directed current loses strength, with a predominance of an onshore-directed current in the upper part of the beach. It is important to notice that as the undertow loses strength, water fluxes in this zone of the beach are less intense compared to water fluxes in elevations above MSHTL.

Most of the deposition occurred at the beginning of the inundation. Using scenario k. as an example, we extracted information from a profile and a point in space, as highlighted in Figure 11. Results show that deposition occurred mostly between 2:00 and 4:00 hours, which is also the period when water levels reached sufficient elevation to inundate the flat. Between 2:00 and 4:00, values of wave height found in the flat are in the order of 0.1-0.2 meters. After 4:00, the increase of water levels reduces wave dissipation and, in turn, allow wave height in the order of 0.5-0.6 meters on the flat. This suggests that the deposition is a wave-driven process, which may be associated with wave breaking. As water starts to inundate the flat, wave breaking start to erode the beach. As the breaking evolve as an onshore-directed water flux, it transports the eroded sediment in the down-wave direction. This process occurs for the period in which water depth is small enough to dissipate most of the wave energy, which is supported by the really small waves on the flat. As water depth increase, there is a reduction of wave dissipation, that in turn reduces the sediment transport capacity.

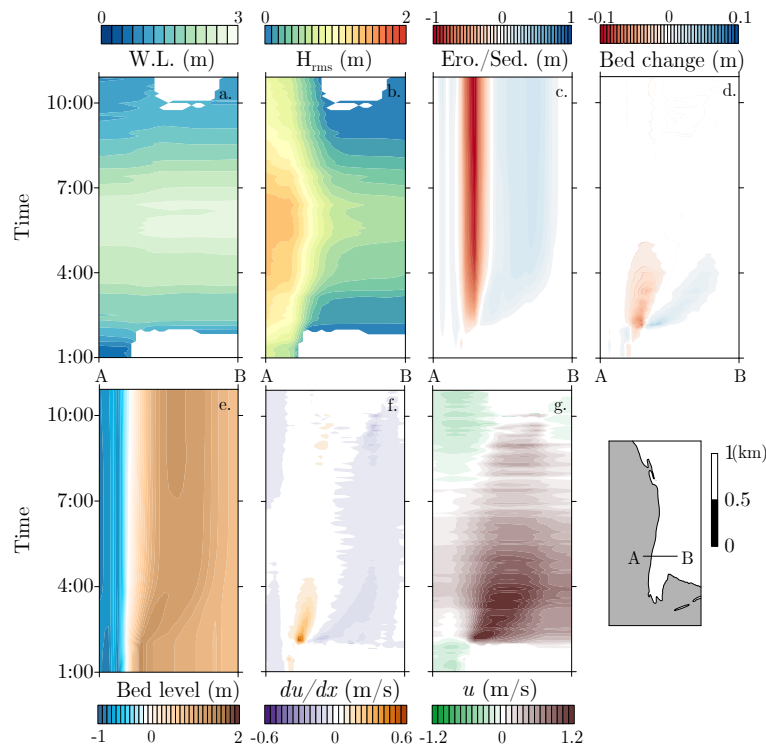


Figure 11. Evolution of hydrodynamic and morphological characteristics along the transect A-B taken from scenario k. Y-axis represent the time, whereas the X-axis represent the distance between A and B (left to right), shown on the small reference plot. Variables shown are: local water level relative to NAP (a.), Wave height (b.), cumulative bed level change (c.), bed level change (d.), Bed level (e.), cross-shore convergence of u (f.) and zonal components (u) of the flow (g.)



Convergence values of the cross-shore current component (u) help to further explain the mechanism of deposition. Positive values of du/dx occur immediately at the beginning of the inundation phase, as water level reaches values of 1.8 meters (Figure 12). Positive values, which relate to divergence of currents, can be related to immediate acceleration of water fluxes due to wave breaking in the cross-shore direction. Moreover, divergence of currents will also lead to erosion of the beach. As water starts to inundate the upper part of the beach, wave-driven water fluxes start to decelerate in the cross-shore direction, resulting in a zone of convergence, leading to deposition.

Results show that most sediment is eroded from positions below the MSHTL (Figure 13). Using the transect A-B from scenario k as example, results show that median values of elevation where sediment was eroded is 0.61 meters, whereas sediment was deposited on a median elevation of 1.34. Moreover, 85% of the deposition over the whole period occurred in elevations above the MSHTL, whereas 34% of the erosion occurred in elevations above MSHTL. That suggests that sediment tend to be transported from a regularly hydrodynamically active zone (i.e. below MSHTL) to a zone with a sparser occurrence of hydrodynamic processes (i.e. above MSHTL). Moreover, results show that accretion also occurred in areas below 0 meters. This deposition occurs mainly before the inundation of the sand-flat and is mainly associated to the offshore-directed current which develops before the inundation phase. Sediment is eroded from the upper beach and transported towards the sea, being then deposited in regions below mean sea level.

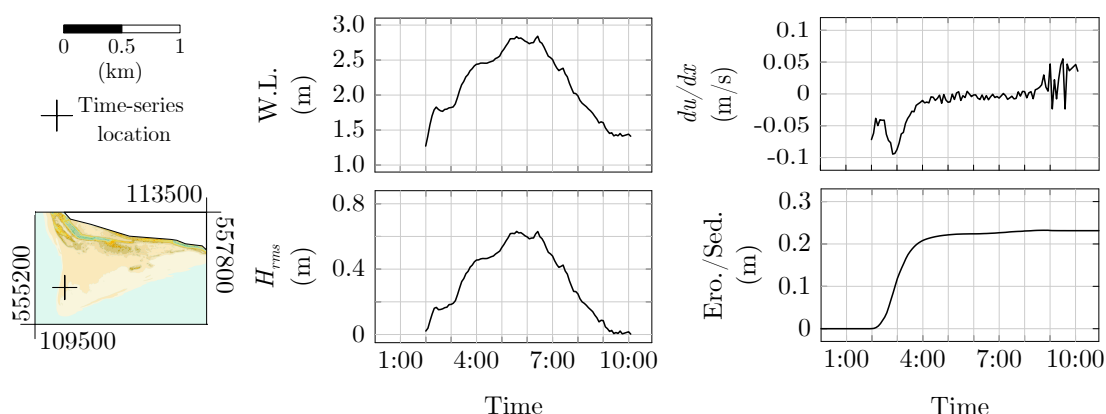


Figure 12. Time series of hydrodynamic and morphological characteristics extracted from scenario k.

Using the volume deposited on the sand flat from the simulations, it is possible to make an estimate of the amount of sediment deposited on the sand flat in reality using regression techniques. Using both the initial water level and wave height from the simulations as predictors, we could pair the results with measured water levels and wave height in reality. Estimates of sand being deposited on the sand flat shows that, between 1997-2017 (i.e. dates which we have LiDAR data and dune volume estimates), the amount of sand predicted to be deposited on the sand flat accounts for 67% of the total sand deposited at the dunes (Figure 14). Curves remain similar up to the year of 2007, where a divergency occurs due to a mild period in terms of



storms. The maintenance of the volume increase in the LiDAR data suggests that even though storm-induced deposition may account for large portion of the deposited volume, it is not the only source mechanism of sand for dune growth.

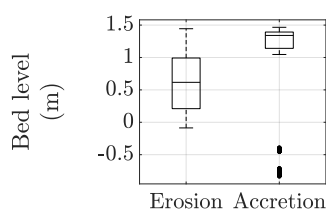


Figure 13. Box plot of the elevation where erosion or accretion occurred extracted from scenario k. as example.

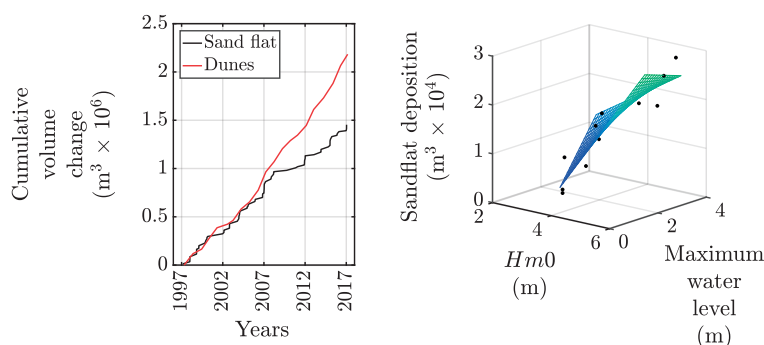


Figure 14. Left: Cumulative volume changes from the dunes using LiDAR data (Dunes) and estimated sand flat deposition using regression model as predictor (Sand). Regression model has been built using simulation results with maximum water level at the boundary and wave height as predictors for deposition. Right: Scatter plot of the regression model used with regression surface.

5 Discussion.

Overall, both elevation survey data and modelling results suggest that: (i) there is a shore-parallel deposition pattern that occurs at the sand-flat in areas above the MSHTL (ii) the deposition can be linked to storm events and (iii) the amount of sediment deposited might have a significant importance for dune growth in the area.

As mentioned by Wijnberg et al. (2017), the magnitude of the sand-flat surface area is in the order of 2km^2 . Considering the total amount of sand accreted at the dunes and considering the sand flat as its only source, the same amount would represent a lowering in the order of 1 meter in height of the sand flat. Considering the stability of the sand flat in a yearly scale, which can be seen through the variance and rate of changes at the sand flat, Wijnberg et al. (2017) suggests that either the sand flat has been continuously replenished by sand or that it is not the main source of sediment for the dunes. Our elevation survey data results suggest that sand deposited above MSHTL can contribute with more than 50% of the sediment supply of the dunes in a yearly



basis. Furthermore, numerical modelling results support that storms may act as a depositional mechanism onto sand-flats, depositing similar shore-parallel supratidal deposits of sand as seen in the elevation data. Also, estimates pairing modelling results and actual data also suggest that cumulative depositions would be on the same order of magnitude of volume changes at the dunes. The potential to contribute to more than half of the yearly average deposited volume in the dunes suggests that, for a sand-flat setting like Texel, the sediment deposited through storm surge flooding can be seen as an important mechanism in terms of sediment exchange between sub-tidal and subaerial zone and, subsequently, dune growth.

Furthermore, storms can also induce another mechanism that might make potential sediment available for the dunes. Results from the field survey related to the washers show that a storm is capable of remobilising the top layer of the sand flat for a great area of the flat. Hoonhout and de Vries (2017) suggested that in a mega-nourishment setting, wind transport would lead to a sorting processes of the sediments at the beach surface that, within a certain period of time, would induce an armouring effect that could reduce the potential of the surface to act as a sediment source. Considering that large parts of the sand-flat remain exposed most of the time, there is a possibility of armouring effects reducing the capacity of the flat to serve as a sediment source. Thus, the occurrence of remobilisation of the top layer after storms would mix sediments from the top layer, making sediment previously armoured to be available again for wind transport. Although possible, to what extent the armouring effect does also occur in a sand-flat setting and what effect this has on the sediment transport towards the dunes remains to further research.

Although modelling results suggest that the amount of sand deposited is directly proportional to storm strength (i.e. storm surge level plus wave energy), data analysis does not show statistical evidence that it happens in reality. This discrepancy may be explained by: the annual time interval of the surveys; cumulative effect of multiple storms before the total dispersion of the deposition of the previous one; the date which the measurement has been taken, since surveys done close to storms would have a higher probability of picturing the shore-parallel deposition pattern; changes in the sand-flat shape between storms, which might lead to slightly non-uniform hydrodynamic forcing in time, thus influencing the potential capacity of sand to be transferred from the sub-tidal to the subaerial zone.

Currently, it is hard to quantify exactly how much sand related to storm deposition or remobilisation of previously deposited sand contributes to dune growth. LiDAR results show that the sediment deposited on the sand flat represent more than half of the sediment necessary to maintain the dune increase at the rates that have been measured. However, being available for transport does not mean that the sediment will actually end up at the dunes, since other hydrodynamic processes (e.g. next storm surge, erosion due to channel migration) may transport it back to the sub-tidal area. Moreover, wind also can transport this sand back to the sub-tidal zone depending on its direction. Furthermore, limiting factors such as surface moisture and lag deposits can reduce considerably the capacity of the wind to transport the sand from the sand flat towards the dunes (Delgado-Fernandez and Davidson-Arnott, 2011; de Vries et al., 2012; Bauer et al., 2009; Houser and Ellis, 2013; Duarte-Campos et al., 2018). Thus, synchronisation of capable wind events, bed/grain characteristics and available sediment plays a key role (Houser, 2009). Nevertheless, considering the capacity of sediment deposition suggested by our results together with the dominant wind direction, it is probable that at least part of this sediment contributes to dune growth.



Berm formation and supra-tidal shore-parallel depositional ridges on open coastal beaches have been already related to deposition of sediment related to swash processes (Houser and Ellis, 2013). Several authors exemplify that exchange of sediment between sub-tidal and subaerial zones depend on surf and swash processes during calm conditions or migration of sub-tidal and intertidal bars landward (Houser and Ellis, 2013; Aagaard et al., 2004; Jackson et al., 2004; Houser and Barrett, 2010).

5 Our present research suggests that, for a sand-flat setting, a supra-tidal shore-parallel depositional ridge can also form during a storm surge flooding, inducing the deposition of certain amount of sand that is in the same order of magnitude of the amount of dune volume increase.

6 Conclusions

A sand-flat at the tip of the island of Texel (NL) has been analysed to identify processes and storm properties that cause deposition on the sand-flat during storm-surge flooding and discuss the relation between the supra-tidal deposition and sand supply to the dunes. The case was approached by an integrated analysis of LiDAR surveys, field survey and numerical modelling. Results suggest that supra-tidal deposition of sand is directly proportional to storm surge levels and wave energy, and the amount of sand deposited may account for more than half of the volume deposited at the dunes in a yearly basis. Sediment is mostly eroded from areas below MSHTL and deposited further landward by a wave-driven onshore directed flow. Furthermore, simulation results suggest that most of the deposition occurs at the beginning of the sand-flat inundation and it is controlled by the convergence of the cross-shore component of the wave-driven flow. Furthermore, storms are also capable of remobilising the top layer of sediment of the sand-flat, making fresh sediment available for Aeolian transport if an armouring effect occurred, especially in the west part of the sand-flat. Therefore, in a sand-flat setting, storm surges have the potential of transferring significant amount of sand from the sub-tidal to the supra-tidal zone. This suggests that storms play a significant role supplying sand for the dunes to grow in a sand-flat setting.

10
15
20

Code and data availability. Data used related to long-term Dutch monitoring program can be found at opendap.deltares.nl. Remaining datasets and code are available upon request from Filipe Galiforni Silva (f.galifornisilva@utwente.nl).

Competing interests. The authors declare that they have no conflict of interest

Acknowledgements. This research forms a component of the CoCoChannel project (Co-designing Coasts using natural Channel-shoal dynamics), which is funded by Netherlands Organization for Scientific Research, Earth Sciences division (NWO-ALW), and co-funded by Hoogheemraadschap Hollands Noorderkwartier. We further wish to acknowledge Rijkswaterstaat and KNMI for making their valuable bathymetric and topographic data sets freely available, as well as the water level, wave and wind data. Furthermore, we would like to thank Prof. Dr. Dano Roelvink for his help and discussions on the application of the XBeach model.

25



References

- Aagaard, T.: Sediment supply to beaches: Cross-shore sand transport on the lower shoreface, *Journal of Geophysical Research: Earth Surface*, 119, 913–926, 2014.
- Aagaard, T., Nielsen, J., Jensen, S. G., and Friderichsen, J.: Longshore sediment transport and coastal erosion at Skallingen, Denmark, *Geografisk Tidsskrift-Danish Journal of Geography*, 104, 5–14, <https://doi.org/10.1080/00167223.2004.10649499>, 2004.
- 5 Anthony, E. J.: Storms, shoreface morphodynamics, sand supply, and the accretion and erosion of coastal dune barriers in the southern North Sea, *Geomorphology*, 199, 8–21, <https://doi.org/10.1016/j.geomorph.2012.06.007>, 2013.
- Anthony, E. J., Vanhee, S., and Ruz, M. H.: Short-term beach-dune sand budgets on the north sea coast of France: Sand supply from shoreface to dunes, and the role of wind and fetch, *Geomorphology*, 81, 316–329, <https://doi.org/10.1016/j.geomorph.2006.04.022>, 2006.
- 10 Bauer, B. O. and Davidson-Arnott, R. G. D.: A general framework for modeling sediment supply to coastal dunes including wind angle , beach geometry , and fetch effects, *Geomorphology*, 49, 89–108, [https://doi.org/10.1016/S0169-555X\(02\)00165-4](https://doi.org/10.1016/S0169-555X(02)00165-4), 2002.
- Bauer, B. O., Davidson-Arnott, R. G. D., Hesp, P. a., Namikas, S. L., Ollerhead, J., and Walker, I. J.: Aeolian sediment transport on a beach: Surface moisture, wind fetch, and mean transport, *Geomorphology*, 105, 106–116, 2009.
- Bochev-Van der Burgh, L., Wijnberg, K., and Hulscher, S.: Decadal-scale morphologic variability of managed coastal dunes, *Coastal Engineering*, 58, 927 – 936, <https://doi.org/https://doi.org/10.1016/j.coastaleng.2011.05.013>, 2011.
- 15 Bochev-van der Burgh, L. M. v., Wijnberg, K. M., and Hulscher, S.: Dune Morphology along a Nourished Coastline, *Journal of Coastal Research*, pp. 292–296, <https://doi.org/10.2307/25737584>, 2009.
- Cohn, N., Ruggiero, P., de Vries, S., and García-Medina, G.: Beach Growth driven by intertidal sandbar welding, in: *Proceedings of Coastal Dynamics 2017*, 2017.
- 20 de Vries, J. V. T.: Dune Erosion during storm surges, Phd thesis, Delft University of Technology, Delft, 2009.
- de Vries, S., Southgate, H. N., Kanning, W., and Ranasinghe, R.: Dune behavior and aeolian transport on decadal timescales, *Coastal Engineering*, 67, 41–53, <https://doi.org/10.1016/j.coastaleng.2012.04.002>, 2012.
- Delgado-Fernandez, I. and Davidson-Arnott, R.: Meso-scale aeolian sediment input to coastal dunes: The nature of aeolian transport events, *Geomorphology*, 126, 217–232, <https://doi.org/10.1016/j.geomorph.2010.11.005>, <http://linkinghub.elsevier.com/retrieve/pii/S0169555X10005088>, 2011.
- 25 S0169555X10005088, 2011.
- Deltares: XBeach Manual, <https://xbeach.readthedocs.io/>, 2018.
- Duarte-Campos, L., Wijnberg, K., and Hulscher, S.: Estimating Annual Onshore Aeolian Sand Supply from the Intertidal Beach Using an Aggregated-Scale Transport Formula, *Journal of Marine Science and Engineering*, 6, 127, <https://doi.org/10.3390/jmse6040127>, 2018.
- Duran-Matute, M., Gerkema, T., De Boer, G. J., Nauw, J. J., and Gräwe, U.: Residual circulation and freshwater transport in the Dutch Wadden Sea: A numerical modelling study, *Ocean Science*, 10, 611–632, <https://doi.org/10.5194/os-10-611-2014>, 2014.
- 30 Eastwood, E., Nield, J., Baas, A., and Kocurek, G.: Modelling controls on aeolian dune-field pattern evolution, *Sedimentology*, 58, 1391–1406, <https://doi.org/10.1111/j.1365-3091.2010.01216.x>, 2011.
- Elias, E. P. L. L. and Spek, A. J. F. v. d.: Dynamic preservation of Texel Inlet, the Netherlands: understanding the interaction of an ebb-tidal delta with its adjacent coast, *Netherlands Journal of Geosciences*, 96, 293 – 317, 2017.
- 35 Elias, E. P. L. L. and Van Der Spek, A. J. F.: Long-term morphodynamic evolution of Texel Inlet and its ebb-tidal delta (The Netherlands), *Marine Geology*, 225, 5–21, <https://doi.org/10.1016/j.margeo.2005.09.008>, 2006.



- Elsayed, S. M. and Oumeraci, H.: Effect of beach slope and grain-stabilization on coastal sediment transport: An attempt to overcome the erosion overestimation by XBeach, *Coastal Engineering*, 121, 179 – 196, 2017.
- Fenster, M. and Dolan, R.: Assessing the impact of tidal inlets on adjacent barrier island shorelines, *Journal of Coastal Research*, 12, 294–310, 1996.
- 5 Fitzgerald, D. M., Penland, S., and Nummedal, D.: Control Of Barrier Island Shape By Inlet Sediment Bypassing: East Frisian Islands, West Germany, *Marine Geology*, 60, 355 – 376, [https://doi.org/https://doi.org/10.1016/0025-3227\(84\)90157-9](https://doi.org/https://doi.org/10.1016/0025-3227(84)90157-9), 1984.
- Hesp, P.: Morphodynamics of incipient foredunes in new south wales, australia, *Developments in Sedimentology*, 38, 325–342, [https://doi.org/10.1016/S0070-4571\(08\)70802-1](https://doi.org/10.1016/S0070-4571(08)70802-1), 1983.
- Hesp, P.: Foredunes and blowouts : initiation , geomorphology and dynamics, *Geomorphology*, 48, 245–268, [https://doi.org/10.1016/S0169-](https://doi.org/10.1016/S0169-1055X(02)00184-8)
10 555X(02)00184-8, 2002.
- Hesp, P. A. and Walker, I. J.: *Coastal Dunes*, vol. 11, Elsevier Ltd., <https://doi.org/10.1016/B978-0-12-374739-6.00310-9>, 2013.
- Hoonhout, B. and de Vries, S.: Field measurements on spatial variations in aeolian sediment availability at the Sand Motor mega nourishment, *Aeolian Research*, 24, 93 – 104, <https://doi.org/https://doi.org/10.1016/j.aeolia.2016.12.003>, 2017.
- Houser, C.: Synchronization of transport and supply in beach-dune interaction, *Progress in Physical Geography*, 33, 733–746, <https://doi.org/10.1177/0309133309350120>, 2009.
- 15 Houser, C. and Barrett, G.: Divergent behavior of the swash zone in response to different foreshore slopes and nearshore states, *Marine Geology*, 271, 106 – 118, 2010.
- Houser, C. and Ellis, J.: Beach and Dune interaction, in: *Treatise on Geomorphology*, edited by Press., A., vol. 10, pp. 267–288, San Diego, 2013.
- 20 Jackson, N. L., Masselink, G., and Nordstrom, K. F.: The role of bore collapse and local shear stresses on the spatial distribution of sediment load in the uprush of an intermediate-state beach, *Marine Geology*, 203, 109–118, [https://doi.org/10.1016/s0025-3227\(03\)00328-1](https://doi.org/10.1016/s0025-3227(03)00328-1), 2004.
- Keijsers, J. G., De Groot, a. V., and Riksen, M. J.: Vegetation and sedimentation on coastal foredunes, *Geomorphology*, 228, 723–734, <https://doi.org/10.1016/j.geomorph.2014.10.027>, 2015.
- McCall, R., de Vries, J. V. T., Plant, N., Dongeren, A. V., Roelvink, J., Thompson, D., and Reniers, A.: Two-dimensional time dependent hurricane overwash and erosion modeling at Santa Rosa Island, *Coastal Engineering*, 57, 668–683, <https://doi.org/10.1016/j.coastaleng.2010.02.006>, 2010.
- 25 Nederhoff, C.: Modeling the effects of hard structures on dune erosion and overwash, Master thesis, Delft University of Technology, Delft, 2014.
- Reichmüth, B. and Anthony, E. J.: Tidal influence on the intertidal bar morphology of two contrasting macrotidal beaches, *Geomorphology*, 90, 101 – 114, 2007.
- 30 Robin, N., Levoy, F., Monfort, O., and Anthony, E.: Short-term to decadal-scale onshore bar migration and shoreline changes in the vicinity of a megatidal ebb delta, *Journal of Geophysical Research*, 114, <https://doi.org/10.1029/2008jf001207>, 2009.
- Roelvink, D., Reniers, A., van Dongeren, A., van Thiel de Vries, J., McCall, R., and Lescinski, J.: Modelling storm impacts on beaches, dunes and barrier islands, *Coastal Engineering*, 56, 1133–1152, <https://doi.org/10.1016/j.coastaleng.2009.08.006>, 2009.
- 35 Ruessink, B. G. and Jeuken, M. C. J. L.: Dunefoot dynamics along the Dutch coast, *Earth Surface Processes and Landforms*, 27, 1043–1056, <https://doi.org/10.1002/esp.391>, 2002.
- Sherman, D. J. and Bauer, B. O.: Dynamics of beach-dune systems, *Progress in Physical Geography*, 17, 413–447, <https://doi.org/10.1177/030913339301700402>, 1993.



- Short, A. D. and Hesp, P. A.: Wave, beach and dune interactions in southeastern australia, *Marine Geology*, 48, 259–284, 1982.
- Silva, F. G., Wijnberg, K. M., de Groot, A. V., and Hulscher, S. J. M. H.: The influence of groundwater depth on coastal dune development at sand flats close to inlets, *Ocean Dynamics*, <https://doi.org/10.1007/s10236-018-1162-8>, 2018.
- Silva, F. G., Wijnberg, K. M., de Groot, A. V., and Hulscher, S. J.: The effects of beach width variability on coastal dune development at
 5 decadal scales, *Geomorphology*, 329, 58–69, <https://doi.org/10.1016/j.geomorph.2018.12.012>, 2019.
- van Heteren, S., Oost, A. P., van der Spek, A. J. F., and Elias, E. P. L.: Island-terminus evolution related to changing ebb-tidal-delta configuration: Texel, The Netherlands, *Marine Geology*, 235, 19–33, <https://doi.org/10.1016/j.margeo.2006.10.002>, 2006.
- van Puijenbroek, M. E., Limpens, J., de Groot, A. V., Riksen, M. J., Gleichman, M., Slim, P. A., van Dobben, H. F., and Berendse, F.: Embryo
 dune development drivers: Beach morphology, growing season precipitation, and storms, *Earth Surface Processes and Landforms*, 4144,
 10 <https://doi.org/10.1002/esp.4144>, 2017.
- Vet, P. D.: Modelling sediment transport and morphology during overwash and breaching events, Master thesis, Delft University of Technology, Delft, 2014.
- Wijnberg, K. M., van der Spek, A. J., Silva, F. G., Elias, E., van der Wegen, M., and Slinger, J. H.: Connecting subtidal and subaerial sand transport pathways in the Texel inlet system, in: *Coastal Dynamics Proceedings*, 235, pp. 323–332, 2017.